Title: Vaccinia virus BBK E3 ligase adaptor A55 targets importin-dependent NF-κB activation and inhibits $CD8^+$ T-cell memory

Authors: Mitchell A. Pallett, Hongwei Ren, Rui-Yao Zhang, Simon R. Scutts, Laura Gonzalez[2], Zihan Zhu, Carlos Maluquer de Motes[1] and Geoffrey L. Smith[#]

Corresponding Author: Geoffrey L. Smith

Affiliation:

Division of Virology, Department of Pathology, University of Cambridge, Cambridge, United Kingdom

Current address:

1. Department of Microbial Sciences, University of Surrey, Guildford, United Kingdom
2. Institute for Research in Biomedicine, University of Barcelona, Spain.

Funding: Wellcome Trust grant 090315

Abstract

Viral infection of cells is sensed by pathogen recognition receptors that trigger an anti-viral innate immune response and consequently viruses have evolved countermeasures. Vaccinia virus (VACV) evades the host immune response by expressing scores of immunomodulatory proteins. One family of VACV proteins are the BTB-BACK domain containing, Kelch-like (BBK) family of predicted cullin-3 E3 ligase adaptors: A55, C2 and F3. Previous studies demonstrated that gene *A55R* encodes a protein that is non-essential for VACV replication yet affects viral virulence *in vivo*. Here we report that A55 is an NF-κB inhibitor acting downstream of IκBα degradation, preventing gene transcription and cytokine secretion in response to cytokine stimulation. A55 targets the host importin α1 (KPNA2), acting to reduce p65 binding and its nuclear translocation. Interestingly, whilst A55 was confirmed to co-precipitate with cullin-3 in a BTB-dependent manner, its NF-κB inhibitory activity mapped to the Kelch domain, which alone is sufficient to co-precipitate with KPNA2 and inhibit NF-κB signalling. Intradermal infection of mice with a virus lacking *A55R* (vΔA55) increased VACV-specific $CD8^+$ T-cell proliferation, activation, and cytotoxicity in comparison to the WT virus. Furthermore, immunisation with vΔA55 induced increased protection to intranasal VACV challenge compared to control viruses. In summary, this report describes the first target of a poxvirus-encoded BBK protein and a novel mechanism for DNA virus immune evasion, resulting in increased $CD8^+$ T-cell memory and a more immunogenic vaccine.

Importance

NF-κB is a critical transcription factor in the innate immune response to infection and in shaping adaptive immunity. The identification of host and virus proteins that modulate the induction of immunological memory is important for improving virus-based vaccine design and efficacy. In viruses, the expression of BTB-BACK Kelch-like (BBK) proteins is restricted to poxviruses and conserved within them, indicating the importance of these proteins for these medically important viruses. Using vaccinia virus (VACV), the smallpox vaccine, we report that the VACV BBK protein A55 dysregulates NF-κB signalling by disrupting the p65-importin interaction, thus preventing NF-κB translocation and blocking NF-κB-dependent gene transcription. Infection with VACV lacking A55 induces increased VACV-specific $CD8^+$ T-cell memory and better protection against VACV challenge. Studying viral immunomodulators therefore expands not only our understanding of viral pathogenesis and immune evasion strategies, but also understanding of the immune signalling cascades controlling anti-viral immunity and the development of immune memory.

Introduction

Virus infection is sensed by pattern recognition receptors (PRRs) that detect pathogen associated molecular patterns (PAMPs) and this triggers an innate immune response to restrict viral replication and spread. PRR-ligand binding leads to intracellular phospho-kinase signalling cascade(s) and activation of specific inflammatory transcription factors including nuclear factor kappa-light chain-enhancer of activated B cells (NF-κB), interferon regulatory factor 3, 7 or 9 (IRF3/7/9) and signal transducer and activator of transcription (STAT) proteins (1). Activation of these transcription factors controls the host innate immune response by the direct and specific transcriptional regulation of pro-inflammatory and anti-viral genes. Canonical NF-κB signalling mediated via tumour necrosis factor receptor (TNFR), interleukin-1 receptor (IL-1R), retinoic acid-induced gene 1 (RIG-I)-like receptors (RLRs) and DNA sensing converges at the inhibitor of kappa B kinase (IKK) (1). Phosphorylated IKKβ in turn phosphorylates the inhibitor of NF-κB subunit alpha (IκBα) that induces its cullin-1/β-TrCP-dependent degradation (2). Under normal conditions IκBα tethers NF-κB in the cytoplasm preventing NF-κB dependent gene transcription. Free NF-κB binds to importin α1-4 (karyopherin subunit alpha (KPNA) 1-4)/importin β and translocates into the nucleus (3–6) where, following phosphorylation dependent CBP/P300- acetylation (7), it upregulates NF-κB dependent gene transcription. NF-κB-induced cytokines and chemokines then promote inflammation and immune cell recruitment to clear infection.

During their evolution viruses have acquired proteins to counteract the host immune response. A prototypical example is vaccinia virus (VACV), the live vaccine used to eradicate smallpox. VACV is a member of the genus *Orthopoxvirus* of the *Poxviridae,* a family of large double-stranded DNA viruses that replicate in the cytoplasm. To evade the host immune response VACV encodes a plethora of immunomodulatory proteins including more than 10 inhibitors of NF-κB activation that function at different stages in the pathway (8). For instance, protein B14 targets IKKβ to prevent IκBα phosphorylation and degradation and subsequent p65 nuclear translocation (9). K7 was reported to co-precipitate with TRAF6

and IRAK2 to suppress TLR-dependent NF-κB activation (10), and A49 blocks β-TrCP-mediated degradation of phosphorylated IκBα via molecular mimicry (11). Although ten VACV inhibitors of NF-κB have been described, others exist because a virus lacking all these inhibitors still inhibited NF-κB activation (12). Ectromelia virus, a related orthopoxvirus that causes mousepox, encodes several inhibitors of NF-κB, including protein EVM150 (13) that shares 93 % amino acid identity with VACV strain Western Reserve (WR) protein A55. A55 belongs to the BBK (Broad-Complex, Tram-Trac and Bric a Brac (BTB) and C-terminal Kelch (BACK) family of proteins (14). Interestingly, outside mammals only poxviruses encode Kelch-like proteins (15).

BTB-Kelch proteins are substrate-specific adaptors for the cullin-3 ubiquitin–ligase complex and regulate modification and/or degradation of various proteins by ubiquitylation (16). Several orthopoxvirus BBK proteins co-precipitate with cullin-3 (15). The N-terminal BTB domain is essential for cullin-3 interaction and contains a conserved tertiary structure consisting of five α-helices with A1/2 and A4/5 forming α-helical hairpins, and three β-strands (B1/B2/B3) forming a β-sheet. The B1/B2/A1/A2/B3 region is connected to the A4/A5 region by helix A3 and a variable linker region (17). The Kelch motif is a segment of 44–56 amino acids with low overall sequence identity but eight key conserved residues, including four hydrophobic residues followed by a double glycine element, separated from two characteristically spaced aromatic residues, tyrosine and tryptophan (18). Each Kelch motif represents one β-sheet blade, and several (4-7) of these repeats can form a beta-propeller (19) and a substrate binding domain. Traditionally, the Kelch domain acts as the E3 ligase substrate receptor and therefore controls substrate specificity. BBK proteins through variation within their Kelch domain modulate a wide range of cellular processes including actin association/cytoskeleton organisation, cell morphology, innate immunity, and gene expression (18). For example, KLHL20 targets IKKβ to downregulate NF-κB signalling (20), while KLHL12 disrupts Wnt-β-catenin signalling through the recruitment of Dishevelled to the cullin-3 E3 ligase complex and its subsequent ubiquitylation and degradation (21).

VACV encodes three BBK proteins, A55, C2 and F3 and one BTB-only protein C5 (14). Like many other VACV immunomodulators, the VACV BBKs are expressed early during infection (22) and share low amino acid identity. This is 23.5 % between A55 and F3, and 18.7 % and 18.3 % between C2 and A55 and F3, respectively. Previous studies have demonstrated that the genes *A55R*, *F3L* and *C2L* encode proteins that are non-essential for virus replication yet affect virulence in an intradermal mouse model (23–25). C2 and F3 modulate immune cell recruitment and proliferation *in vivo* (24, 25). Although the virus lacking gene *A55R* (vΔA55) has altered virulence, how A55 affects virulence, and whether it recruits cullin-3 or inhibits inflammatory signalling remain unknown. Thus, we investigated the effect of A55 on host innate immune signalling pathways *in vitro* and *in vivo*, and whether this modulated the immune response *in vivo* and/or made for a more protective vaccine.

Results

A55 specifically inhibits NF-κB activation *in vitro*

Due to the conservation between EVM150 and A55 and because other NF-κB inhibitors exist in the VACV genome (12), a role for A55 in NF-κB signalling was investigated. HEK293T's were co-transfected with a plasmid expressing A55 and plasmids encoding NF-κB-Luc and pTK-Renilla. Cells were stimulated with TNFα or IL-1β or left unstimulated and Firefly luciferase was measured alongside Renilla as an internal control. Empty vector (EV) and the human BBK KLHL12 were used as negative controls, while B14 was included as a known NF-κB inhibitor. A55 expression inhibited NF-κB activity in response to both IL-1β and TNFα compared to the EV and KLHL12 controls (Fig. 1A-B) in a dose-dependent manner (Fig. 1C). A55 also inhibited expression of endogenous NF-κB-responsive genes in response to TNFα-stimulation. For instance, transcription of IL-8 (measured by RT-qPCR) and secretion of CXCL10 (measured by ELISA) were both inhibited by A55 (Fig. 1D-E). In contrast, A55 did not inhibit the JAK-STAT (ISRE-luc) or activator protein 1 (AP-1) promoter activity in response to interferon (IFN)α or phorbol myristic acid (PMA), respectively (Fig. 1F-G). VACV protein C6 inhibited IFNα-stimulated ISRE activity as reported (Fig. 1G) (26). The ability of A55 to inhibit both IL-1β and TNFα-induced stimulation of NF-κB signalling suggested that it acts at or below TAK1 phosphorylation where the IL-1R and TNFR pathways converge.

Inhibitory activity of A55 is mapped to NF-κB activation downstream to IκBα degradation

The NF-κB pathway can be activated by overexpression of proteins acting at specific stages. Thus, to map where A55 inhibits the pathway, plasmids encoding TRAF6, TRAF2, TAK1/TAB1, IKKβ or p65 were co-transfected into HEK293Ts along with pcDNA4/TO-nTAP-co*A55R*. Pathway activation was measured by NF-κB-luciferase expression as above. EV and KLHL12 or B14 were used as negative and positive controls, respectively. B14 inhibited at IKKβ (9) (Fig. 2A-D), whilst KLHL12 was not inhibitory (Fig. 2A-E). A55 expression

inhibited NF-κB activity in response to TRAF2, TRAF6, TAK1, IKKβ and p65 (Fig. 2A-E), and in the latter case the degree of inhibition increased with greater expression of A55 (Fig. 2E). Therefore, A55 acts at the level of p65 or downstream.

Under resting conditions IκBα tethers NF-κB in the cytoplasm but upon stimulation IκBα is phosphorylated by IKKβ, ubiquitylated and degraded by the β-TrCP/cullin-1 E3 ligase complex and proteosome (27). Free p65 phosphorylated at S536 translocates into the nucleus where it undergoes phosphorylation at S276. This facilitates recruitment of p-RNAP II and p300 (7) and formation of the enhancersome to initiate gene transcription. To map the inhibitory mechanism of A55 further, HEK293T-REx cell lines with EV or vectors expressing B14 or A55 were stimulated with TNFα and IκBα levels were analysed. As expected, B14 inhibited TNFα-induced degradation of IκBα (Fig. 3A-B). However, although expression levels of A55 and B14 were similar, A55 did not prevent IκBα degradation (Fig. 3A-B). Consistent with reporter gene assays, this indicated that A55 acted at or below p65 release. Phosphorylation is key to the transcriptional activity of p65. To determine if A55 regulates phosphorylation of p65, HEK293T-REx cells expressing A55 were stimulated with TNFα and the levels of p-p65 S536 and S276 were analysed. While p-p65 S536 levels were comparable, A55 abrogated S276 phosphorylation (Fig. 3C), which is a nuclear event (7). This suggests that A55 may inhibit S276 phosphorylation directly, or indirectly by preventing nuclear translocation of p65.

To explore whether A55 inhibits nuclear translocation of p65, HeLa cells transfected with Flag-tagged EV, B14, A55 or C6 were stimulated with TNFα and the subcellular localisation of p65 was analysed by immunofluorescence (Fig. 4A). Cells were co-stained with anti-Flag and p65, and DAPI to stain DNA, and the number of cells exhibiting nuclear exclusion of p65 were numerated (Fig. 4B). As expected, almost 100% of the EV untreated cells exhibited nuclear exclusion of p65 in comparison to 10% of EV-stimulated cells (Fig. 4B) and B14 prevented nuclear translocation of p65, while protein C6 did not (Fig. 4B). In comparison, A55 inhibited translocation of p65 in 62% of transfected cells following stimulation (Fig. 4B).

Collectively, this maps the inhibitory activity of A55 prior to nuclear translocation of free NF-κB but after IκBα degradation.

A55 targets importins to inhibit NF-κB activation

The nuclear translocation of NF-κB p65 is regulated by importin-α 1-4/importin-β shuttling, dependent upon cell type and stimulus (3–5). To determine if A55 targets the nuclear importins the interaction of A55 and importins was investigated following immunoprecipitation of Flag-tagged KPNA1, 2 or 3 from transfected HEK293Ts that were infected with WT VACV WR. Co-immunoprecipitation (co-IP) of A55 was tested using an A55 specific antibody (23). A55 co-precipitated with KPNA2, but not KPNA1 or 3, whereas C6 was not co-precipitated (Fig. 5A). Consistent with this, endogenous KPNA2, but not KPNA1, co-precipitated with transfected Flag-tagged A55 (Fig. 5B). KPNA2 is required for p65 translocation, and therefore the interaction of p65 and KPNA2 was investigated in the presence of A55 or B14. Transfected HA-p65 was immunoprecipitated and the levels of co-precipitated KPNA2 were reduced in the presence of A55 (Fig. 5C) suggesting A55 may block interaction of KPNA2 and p65. As A55 is a predicated BBK E3 ligase adaptor, the levels of KPNA2 following infection with the WT VACV strain WR (vA55), a mutant lacking gene *A55R* (vΔA55), or the revertant virus with *A55R* inserted back into vΔA55 and under its endogenous promoter were investigated. Notably, the levels of KPNA2 did not alter during infection or transfection (Fig. 5D).

A55 inhibits NF-κB in a Kelch-dependent manner independent of cullin-3 binding

Typically, BBKs recruit cullin-3 via their BTB domain and their substrates to the cullin-3 E3 ligase complex via their C-terminal Kelch domain. Therefore, a possible interaction between A55 and cullin-3 was investigated and this showed that endogenous cullin-3 co-precipitated with A55, but not with B14 (Fig. 6A). This interaction was confirmed by reciprocal IP of overexpressed Myc-tagged cullin-3 or cullin-5 (Fig. 6B). Subdividing A55 into its BTB and Kelch domain (Fig. 6C) showed that precipitation of endogenous cullin-3 was achieved by

193 the BTB domain but not Kelch domain of A55 (Fig. 6D). In contrast, the Kelch domain was
194 sufficient to co-IP endogenous KPNA2 (Fig. 6E). To determine if the Kelch domain mediated
195 inhibition of NF-κB activation, HEK293T-REx cells expressing the full length A55 or the BTB-
196 BACK or Kelch domains separately were stimulated with IL-1β or TRAF6 co-transfection and
197 NF-κB luciferase activity was measured. Despite higher levels of BTB-BACK expression
198 (Fig. 6G) only the Kelch domain inhibited IL-1β- and TRAF6-induced NF-κB activation (Fig.
199 6F). We next tested if either domain was sufficient to prevent NF-κB p65 nuclear
200 translocation. HeLa cells transfected with Flag-tagged C6, A55, A55 BTB or A55 Kelch were
201 stimulated with TNFα and the subcellular localisation of p65 was analysed by
202 immunofluorescence as before. Interestingly, both domains alone appeared to inhibit p65
203 translocation following TNFα stimulation as efficiently as full length A55 (Fig. 7A-B).
204 However, the inhibitory activity of A55 BTB-BACK correlated with induction of cellular
205 vacuolarisation (Fig. 7C) compromising the conclusion that this was indirect inhibition by
206 BTB-BACK. Thus, A55 can inhibit NF-κB activation in a Kelch-dependent and cullin-3-
207 independent manner.

208 **A55 inhibits $CD8^+$ T-cell proliferation and activation in the acute phase of infection**

209 The potential role of A55 as an immunomodulator was investigated next by measuring the
210 immune cell number and activation status, as well as immunological memory in C57BL/6
211 mice infected intradermally with vA55, vΔA55 and vΔA55Rev (28, 29).

212 As expected, the lesion size was increased upon infection with vΔA55 compared to control
213 viruses (data not shown) (23). On day 7 p.i. the absolute cell number of immune cells in the
214 spleen (Fig. 8A) and draining lymph nodes (DLN) (Fig. 8B) were counted. The total splenic
215 and DLN cell number, and $CD8^+$ T-cells and macrophages in these organs, were
216 significantly increased during infection with vΔA55 compared to control viruses, while no
217 significant changes were observed for $CD4^+$ T-cells, neutrophils or NK cells (Fig. 8A-B).
218 $CD8^+$ T-cells also showed enhanced activation (increased CD69 expression) at day 7 p.i.
219 (Fig. 8C-D) and this correlated with increased VACV-specific $CD8^+$ T-cells at day 7 and 28

p.i. (Fig. 8E). In contrast, no increase in NK cell or $CD4^+$ T-cell activity was observed (Fig. 8C-D). Interestingly, the increase in $CD8^+$ T-cell activation upon infection with vΔA55 was still apparent at day 28 p.i (Fig. 8C-E) whereas T cell activation in the WT had returned to basal level. Therefore, we tested if loss of A55 enhanced $CD8^+$ T-cell memory and if so, if immunisation with vΔA55 provides better protection to challenge.

A55 deletion enhances $CD8^+$ T-cell memory and provides protection to VACV challenge

Strong $CD8^+$ T-cell immunological memory is desirable following vaccination (30). To test if A55 modulates immunological memory the killing activity of splenic $CD8^+$ T-cells and NK cells was assessed at day 28 p.i. with vA55, vΔA55 or vΔA55Rev. Killing of VACV-infected EL4 cells by splenic T-cells isolated 28 days p.i. was significantly increased for all three infected groups versus mock control (Fig. 9A). EL4-killing was also greater with $CD8^+$ T-cells isolated from mice immunised with vΔA55 in comparison to control viruses (Fig. 9A). Notably T-cell mediated killing was reduced to basal levels by the addition of an anti-CD8 antibody, showing cytolysis was $CD8^+$ T-cell specific (Fig. 9B). In contrast, no differences between the vA55 or vΔA55 groups were observed in the ability of NK cells to kill VACV-infected P815 cells following immunisation (Fig. 9A).

To test if vΔA55 makes for a better vaccine, mice infected intradermally with vA55, vΔA55 or vA55Rev were challenged intranasally at day 28 p.i. with vA55. Weight loss and viral titres in the lungs were quantified on days 1 and 4 p.i. Weight loss was significantly reduced from day 3 to day 7 p.i. in vΔA55 immunised mice compared to control groups (Fig. 9C). This was accompanied by a decrease in viral titre in the lungs of vΔA55 immunised mice at day 4 p.i. (Fig. 9D). Taken together these data show that vΔA55 immunised mice are better protected following intranasal challenge and clear viral infection quicker, making for a more efficacious vaccine.

Discussion

During evolution with their hosts, viruses have evolved strategies to evade or suppress the host immune system. The study of virus-encoded proteins that modulate the immune response (immunomodulators or immunevasins) has increased our understanding of not only virus immune evasion and pathogenesis, but also of cellular signalling pathways and regulators of the immune response to infection. VACV encodes scores of immunomodulators and a mutant virus lacking one of these, called A55, increased immunopathology following intradermal infection (23). This observation, and the report that the orthologue of A55 in ectromelia virus, EVM150, inhibited NF-κB (13), led us to investigate the function of A55 further, and the consequence of A55 expression on the NF-κB signalling pathway *in vitro* and the immune response to infection *in vivo*. This report shows A55 targets the cellular importin KPNA2 to dysregulate p65 translocation and restrict NF-κB activation. Furthermore, immunisation with a virus lacking A55 induced a stronger $CD8^+$ T-cell response to VACV and better protection against VACV challenge.

Consistent with a report on EVM150 (13), data presented show that A55 inhibits cytokine expression and NF-κB-luciferase activity in response to TNFα and IL-1β, by preventing p65 translocation but without affecting IκBα levels. This suggested a possible modulation of cellular factors needed for p65 translocation. Consistent with this, A55 co-precipitated with KPNA2, part of the importin complex. Further the interaction seen between KPNA2 and p65 was reduced in the presence of A55, indicating that A55 may disrupt KPNA2-p65 complex formation to inhibit p65 translocation. This observation is relevant to understanding which KPNAs control NF-κB p65 translocation.

Humans encode a family of importins of which KPNA1-4 and KPNA6 are implicated in regulating NF-κB signalling. The interaction of KPNA1-3 with NF-κB was identified from an *in vitro* screen using importins purified from bacteria (5), and an interaction of KPNA2-4 with p65 was observed both *in vitro* and *in vivo*, and the KPNA2/p65 interaction was NLS-dependent (4). Conversely, KPNA2/p65 binding was not observed using recombinant protein

from insect cells, and the authors suggested that KPNA3/4 interaction is more biologically relevant (4). However, this evidence may only suggest that KPNA2 does not interact directly with p65 in the absence of pathway stimulation or post-translation modification (4), and KPNA2/p65 binding was enhanced following TNFα stimulation (4). An siRNA screen of the impact of importins on p65 translocation following TNFα stimulation indicated that KPNA2 and KPNA6 contribute the most (3). More recently siRNA mediated knockdown of KPNA2 was shown to impair p65 translocation and NF-κB-dependent gene expression in rat pancreatic Acinar cells (6). Collectively, the literature suggests multiple importins regulate p65 translocation, with KPNA2 playing a leading role. KPNA redundancy may explain why A55-mediated inhibition of p65 translocation is incomplete, and why its inhibition is less efficient than B14, which targets IKKβ (9), or A49, which targets β-TrCP (11).

Targeting of importins to dysregulate cellular signalling has been reported for RNA viruses (31–34). For instance, Japanese encephalitis virus NS5 targets KPNA2-4, with binding of KPNA3/4 preventing IRF3 translocation (32). Hepatitis C virus NS3/4A restricts IRF3 and NF-κB translocation by targeting KPNAB1 (33), and Hantaan virus nucleocapsid protein inhibits p65 translocation and co-precipitated with overexpressed KPNA1, 2 and 4 (34). However, this report is the first describing specific targeting of KPNA2 to disrupt p65-KPNA2 complex formation and subsequently NF-κB signaling and reinforces the importance of KPNA2 in NF-κB translocation. A55 lacks a canonical NLS and is cytoplasmic, and therefore is unlikely to be a KPNA2-dependent cargo, but rather functions in the cytoplasm. Whilst targeting KPNA2 reduces NF-κB signalling, it may also have other consequences on nuclear shuttling that may contribute to the *in vivo* phenotype of vΔA55. The A55 N-terminal BTB domain, which binds cullin-3 may also contribute to this phenotype.

Although the inhibition of NF-kB activation by A55 depends on the A55 Kelch domain and is independent of cullin-3 binding, the BTB-BACK domain likely also has an important function. To start to address this, the co-crystal structure of the A55 BTB-BACK domain bound to cullin-3 was determined and revealed an overall interaction that is conserved between cullin-

3 and other cellular binding partners such as KLHL3, a human BTB (35). Nonetheless, the affinity of A55 BTB-BACK for cullin-3 was much higher than for other cullin-3 binding partners, suggesting that A55 would be an effective competitor for the interaction of cullin-3 and its binding partners (35).

Data presented here are consistent with that for the ectromelia virus orthologue of A55, EVM150, with one exception. Both proteins co-precipitated with cullin-3 via an N-terminal BTB domain, and both inhibited NF-κB activation in a cullin-3-independent manner. With EVM150, however, inhibition of p65 translocation and NF-κB signalling was reported to require only the BTB domain, and the Kelch domain lacked this inhibitory activity (13). In contrast, the A55 Kelch domain mediated co-precipitation with KPNA2 and inhibition of NF-κB activation, and this fits with inhibition being cullin-3-independent. Discrepancies might reflect precisely where A55 and EVM150 were sub-divided, subtle differences in amino acid composition, or changes in solubility and expression levels of the BTB and Kelch domains. Concerning these possibilities, firstly, we expressed the A55 BTB domain as amino acids 1-251, which includes the BACK and 3-box domain. The Kelch domain was expressed as amino acid 252-565. In contrast, the study of EVM1550 expressed the BTB domain only, lacking both the BACK and 3-box domain. Secondly, we observed that the A55 BTB-BACK domain expressed at higher levels than either the Kelch domain or full-length protein and this was adjusted for the reporter assays by modulating the amount of plasmid transfected. Finally, expression of A55 BTB-BACK induced cellular vacuolarisation, a phenotype associated with cullin-3 depletion (36). Therefore, the apparent inhibitory activity of A55 BTB-BACK, and potentially of EVM150-BTB, may be due to overexpression and cullin-3 saturation leading to inhibition of p65 translocation due to loss of cell viability. Whilst the Kelch domain alone was sufficient to inhibit NF-κB signalling, the ability of A55 to bind cullin-3 might still affect NF-κB signalling during infection, where protein levels may be lower and other viral proteins are present, and particularly *in vivo*, where NF-κB activation needs to be

counteracted in different cell types. The existence and conservation of several poxviral BBKs suggest that they play an important role during infection.

Inflammation and expression of NF-κB-dependent cytokines are important for the development and proliferation of effector and memory T-cell populations (37). Consistent with this, deletion of the NF-κB inhibitor A55 modulated the immune response during acute infection and led to enhanced VACV-specific $CD8^+$ T-cell memory. This is reminiscent of a VACV mutant lacking NF-κB inhibitor N1 causing enhanced $CD8^+$ T-cell memory and effector function (38). However, to confirm that it is the ability of A55 to inhibit NF-κB activation that results in the enhanced CD8+ T-cell memory, rather than other functions of the A55 protein, it will be necessary in the future to study the immunogenicity of a virus expressing a mutant A55 protein that is no longer able to bind to cullin-3. Understanding the signals derived from acute infection that mediate development of immunological memory are key to effective future vaccine design. VACV mutants lacking specific immunomodulators are useful tools to understand the mechanisms underlying and controlling immunological memory, but also suggest ways to produce VACV-based vaccines that induce enhanced $CD8^+$ T-cell memory.

In conclusion, this report shows that VACV protein A55 inhibits NF-κB activation, and is the eleventh VACV encoded NF-κB inhibitor (8). Despite the presence of other NF-κB inhibitors, loss of A55 gives an *in vivo* phenotype leading to enhanced $CD8^+$ T-cell memory and better protection against re-infection. Mechanistically, A55 co-precipitates with KPNA2 via its Kelch domain to disrupt p65-KPNA2 interaction and impair p65 nuclear translocation.

Material and methods

Ethics statement

This work was conducted under license PPL 70/8524 from the UK Home Office according to the Animals (Scientific Procedures) Act 1986.

Cells, plasmids, reagents and viruses

All reagents were purchased from Sigma unless otherwise stated. BSC-1 (ATCC) and HEK293T cells were grown in Dulbecco's Modified Eagle's medium (DMEM) high glucose (Gibco), HeLa cells (ATCC) were grown in MEM (Gibco) and EL4 (H-2b; ATCC) and P815 (ATCC) cells were grown in RPMI (Gibco). All media were supplemented with 10 % foetal bovine serum (FBS; Pan Biotech), non-essential amino acids (NEAA) and 50 µg/ml penicillin/streptomycin (P/S) at 37 ºC in a 5 % CO_2 atmosphere. All plasmids used and those constructed during this study are listed in Table 1. Plasmids were generated using conventional restriction enzyme digest and ligation using the primers with restriction enzyme sites listed in Table 1. VACV strain WR recombinants vA55 (plaque purified wild type), vΔA55 (A55 deletion mutant) and vΔA55Rev (revertant virus with A55R re-inserted into vΔA55) were described (23). Infectious virus titres (plaque-forming units [p.f.u.]/ml) were determined by plaque assay on BSC-1 cells.

HEK293T-REx, pLDT and pCW57 cell line generation

HEK293T-REx cells were constructed using the pcDNA4/TO plasmids in Table 1 along with plasmid pcDNA6-TR encoding the tetracycline inducible promoter repressor. After transfection into HEK293T using LT1 transfection reagent, cells were selected using blasticidin and zeocin, following the manufacturer's instructions (Invitrogen). The pCW57 or pLDT plasmids listed in Table 1, along with the EV as a control, were co-transfected with the packaging (pCMV-PACK) and envelope (pCMV-ENV) plasmids for lentivirus production in HEK293Ts or HEK293T TetR (pLDT-TetR transduced HEK293T), respectively, using LT1 transfection reagent (MirusBio). After 48 h the medium was filtered and transferred to fresh

monolayers of HEK293T cells and 3 d later 2 µg/ml puromycin (Invivogen) was added. Transduction and expression was confirmed by the addition of 2 µg/ml doxycycline and immunoblotting of cell lysates.

Luciferase reporter assay

HEK293T cells were transfected with 100 ng pcDNA4/TO-EV, 100 ng pcDNA4/TO-nTAP-*coA55R,* 25 ng pcDNA4/TO-nTAP-*coA55R-BTB,* 100 ng pcDNA4/TO-nTAP-*coA55R-Kelch*, 100 ng pcDNA3-Flag-*KLHL12*, 20 ng pcDNA3-Flag-co*B14R* (9) or 20 ng pcDNA4/TO-cTAP-*C6L* (39) along with 10 ng of plasmid pTK-Renilla (pRL-TK, Promega) and 45 ng of pLUC-NF-κB (R. Hofmeister, University of Regensburg, Germany), pLUC-AP-1 (Andrew Bowie, Trinity College Dublin) or pLUC-ISRE (Promega) using LT1 transfection reagent (MirusBio Ltd). All conditions were transfected with equal amount of total plasmid DNA by supplementing with pcDNA/TO-EV. Simultaneously, where stated, plasmids encoding TRAF2, TRAF6 (Andrew Bowie, Trinity College Dublin), TAK1 and TAB1, IKKβ (Alain Chariot, University of Leige) or p65 were co-transfected. After 24 h cells were stimulated with 20 ng/ml TNFα, 15 ng/ml IL-1β, 1000 U interferon (IFN)α (all Peprotech) or 10 ng/ml phorbol 12-myristate 13-acetate (PMA) for 6 h. Cells were lysed in Passive lysis buffer (Promega) and Firefly/Renilla luciferase activity was measured using a FLUOstar Omega plate reader (BMG Labtech). Relative luminescence levels were calculated by normalising firefly luminescence to Renilla luminescence and are represented as relative to the non-stimulated EV condition.

RT-qPCR

RNA extraction, cDNA synthesis and RT-qPCR were carried out as described (40). qPCR used primers for *IL-8* (AGAAACCACCGGAAGGAACCATCT and AGAGCTGCAGAAATCAGGAAGGCT) and *GAPDH* (TCGACAGTCAGCCGCATCTTCTTT and ACCAAATCCGTTGACTCCGACCTT).

ELISAs

HEK293T-REx cell lines were starved for 6 h in DMEM without supplements before stimulating for 18 h with 20 ng/ml TNFα. CXCL10 in the medium was measured using CXCL10/IP-10 DuoSet ELISA kit (R&D Systems) and the FLUOstar Omega plate reader (BMG Labtech). Experiments were carried out in triplicate and measured with technical repeats.

Translocation assay and immunofluorescent staining

HeLa cells were transfected with plasmids encoding N-terminal TAP-tagged C6, B14 or A55 using the LT1 transfection reagent (MirusBio). After 24 h cells were starved in DMEM without serum for 3 h, followed by stimulation with 40 ng/ml TNFα for 30 min. Cells were washed 3 times in ice-cold PBS and processed for immunofluorescence staining and imaging as described (39). Rabbit anti-Flag and mouse anti-p65 were used as the primary antibodies and goat anti-rabbit 546 and donkey anti-mouse 488 as the secondary antibodies. Images were analysed using the Zeiss Zen microscope software and ImageJ. Experiments were performed in triplicate and carried out three times. For each repeat, 100 flag-positive cells were counted for each condition and the number of cells showing clear nuclear exclusion of p65 were counted to calculate the percentage.

Co-immunoprecipitation

HEK293T-REx cells were induced with 2 µg/ml doxycycline for 24 h and lysed in either phosphate-buffered saline supplemented with 0.5 % NP40 (IGEPAL CA-630) and protease inhibitor, or RIPA buffer (50 mM Tris pH 8.0, 150 mM NaCl, 0.5 M EDTA, 1 % NP40, 0.5% sodium deoxycholate, 0.1 % SDS supplemented with protease inhibitor) where stated. Proteins were immunoprecipitated as described (39) with M2 Flag-beads, HA-beads or Fastflow G-Sepharose (GE Healthcare) incubated previously with mouse monoclonal anti-Myc-Tag clone 9B11 (CST; #2276) at 1:50. After the final wash, beads were incubated in 4x sample loading dye (LDS; Tris 0.5 M pH 6.8, 40 % glycerol, 6 % SDS, 1 % bromophenol blue and 0.8 % β-mercaptoethanol) and analysed by immunoblotting.

Immunoblotting and Antibodies

Samples were prepared by the addition of LDS, boiled and then separated by electrophoresis in a SDS-polyacrylamide gel in Tris-glycine SDS (TGS) buffer (20 mM Tris, 192 mM glycine, 1 % (w/v) SDS) before transferring to a nitrocellulose membrane (GE Healthcare) in Tris glycine (TG) buffer (20 mM Tris-HCl pH 8.3, 150 mM glycine) using the Turboblot system (BioRAD). Membranes were blocked in 5 % milk in Tris-buffered saline (10 mM Tris, 150 mM NaCl) pH 7.4 with 0.1 % (v/v) Tween-20 (TBS-T) for 60 min before incubating with the primary antibody overnight at 4 ºC. Primary antibodies: rabbit polyclonal anti-KPNA2 (Abcam, ab70160), rabbit polyclonal anti-IκBα (CST, #9242), anti-p65 S536 (CST, S3010S), anti-p65 S276 (Santa Cruz, sc-101749), rabbit monoclonal anti-cullin-3 clone EPR3195 (Abcam, ab108407), anti-Flag (F7425), mouse anti-myc 9B11 (CST, #2276), anti-tubulin (Millipore; 05-829), mouse monoclonal anti-KPNA1 187.1 (Santa Cruz, sc-101292), anti-p65 clone F-6 (Santa Cruz, sc-8008), anti-phospho-IκBα (CST, #9246) and antibodies to VACV proteins rabbit polyclonal anti-C6 (39), or A55 (23), or mouse monoclonal D8 clone AB1.1 (41). Membranes were washed 3 times in TBS-T before incubating with secondary antibodies for 1.5 h. Secondary antibodies were goat anti-rabbit IRDye 800CW (926-68032211; LiCOR) and goat anti-mouse IRDye 608LT (926-68020; LiCOR) or, for immunoprecipitated samples, biotin-anti-mouse light chain followed by streptavidin IRDye 680LT (926-68031; LiCOR) was used. Finally, membranes were washed 3 times in TBS-T, dried and imaged using the LiCOR system and Odyssey software. Densitometry was calculated using ImageJ.

Intradermal mouse model of infection and intranasal challenge experiments

Female C57BL/6 mice 6-8 weeks old (*n*=5), were infected with 5×10^3 p.f.u. in both ear pinnae with VACV strains vA55, vΔA55 and vΔA55Rev that had been purified by sucrose density gradient centrifugation. Lesion size was measured daily with a micrometer until day 21. At day 28 p.i. mice were infected intranasally with 10^7 p.f.u. VACV and their weight measured daily for 7 days.

Isolation of cell populations and staining for flow cytometry

Cells from spleen and lymph nodes were isolated by grinding the organ through a 40 µm nylon cell strainer to create single-cell suspensions. Splenocytes were treated with red blood cell (RBC) lysis buffer to remove contaminating RBCs. Single cell suspensions were stained with fluorescently-labelled antibodies: CD3 (clone 145-2C11), CD4 (GK1.5), CD8 (5H10-1), CD45R (RA-6B2), NK1.1 (PK136), CD69 (H1.2F3), F4/80 (BM8), Ly6G (1A8) and CD16/32 (2.4G2) purchased from BD Biosciences or Biolegend. These antibodies were purified or conjugated with PerCP/cy5.5, FITC, APC/Cy7, APC, PE-Cy7, PE or BV650. Isotype controls were used as negative controls. Live cells were discriminated with a fixable LIVE/DEAD stain (Life Technologies). Stained cells were analysed by flow cytometry on a BD LSR Fortessa (BD Biosciences), and data were analysed with FlowJo software (Tree Star Inc.).

DimerX assay to detect VACV-specific $CD8^+$ T cells

The DimerX assay was performed according to the manufacturer's instructions (BD Biosciences) using H-$2K^b$:Ig fusion proteins and $B8_{20}$ peptide (TSYKFESV), as described (38).

$CD8^+$ T-cell and NK cell killing assay

Cytotoxic T lymphocyte activity was assayed by ^{51}Cr-release assay as described (38). VACV-infected EL4 cells or P815 cells were used as targets for VACV-specific cytotoxic T lymphocyte cell lysis or VACV-specific natural killer (NK) cell cytotoxicity, respectively.

Statistics

All experiments were carried out in triplicate and are representative or an average of at least three independent experiments unless stated. Data are the mean +/- SD, or, for *in vivo* data, +/- SEM. All assays were analysed by unpaired T-test with GraphPad Prism 6 Software where $p<0.05$ = *, $p<0.01$ = **, $p<0.001$ = *** and $p<0.0001$ = ****.

476 **Acknowledgements**

477 We thank Prof. M. Shaw, Mount Sinai, New York for plasmids encoding Flag tagged KPNA1-
478 3, Prof. R.T. Moon, University of Washington Seattle for the plasmid encoding Flag-tagged
479 KLHL12 and Dr. B.J. Ferguson, Department of Pathology, University of Cambridge for
480 critical feedback during the project.

References

1. De Nardo D. 2017. Activation of the Innate Immune Receptors: Guardians of the Micro Galaxy : Activation and Functions of the Innate Immune Receptors. Adv Exp Med Biol 1024:1–35.

2. Yaron A, Hatzubai A, Davis M, Lavon I, Amit S, Manning AM, Andersen JS, Mann M, Mercurio F, Ben-Neriah Y. 1998. Identification of the receptor component of the IkappaBalpha-ubiquitin ligase. Nature 396:590–594.

3. Liang P, Zhang H, Wang G, Li S, Cong S, Luo Y, Zhang B. 2013. KPNB1, XPO7 and IPO8 Mediate the Translocation of NF-KappaB/p65 into the Nucleus. Traffic 14:1132–1143.

4. Fagerlund R, Kinnunen L, Kohler M, Julkunen I, Melen K. 2005. NF-{kappa}B is transported into the nucleus by importin {alpha}3 and importin {alpha}4. J Biol Chem 280:15942–15951.

5. Fagerlund R, Melen K, Cao X, Julkunen I. 2008. NF-kappaB p52, RelB and c-Rel are transported into the nucleus via a subset of importin alpha molecules. Cell Signal 20:1442–1451.

6. Cai Y, Shen Y, Gao L, Chen M, Xiao M, Huang Z, Zhang D. 2016. Karyopherin Alpha 2 Promotes the Inflammatory Response in Rat Pancreatic Acinar Cells Via Facilitating NF-kappaB Activation. Dig Dis Sci 61:747–757.

7. Christian F, Smith EL, Carmody RJ. 2016. The Regulation of NF-Kappa-B Subunits by Phosphorylation. Cells 5:12. doi:10.3390/cells5010012.

8. Smith GL, Benfield CT, Maluquer de Motes C, Mazzon M, Ember SW, Ferguson BJ, Sumner RP. 2013. Vaccinia virus immune evasion: mechanisms, virulence and immunogenicity. J Gen Virol 94:2367–2392.

9. Chen RA, Ryzhakov G, Cooray S, Randow F, Smith GL. 2008. Inhibition of IkappaB

kinase by vaccinia virus virulence factor B14. PLoS Pathog 4:e22.

10. Schroder M, Baran M, Bowie AG. 2008. Viral targeting of DEAD box protein 3 reveals its role in TBK1/IKKepsilon-mediated IRF activation. EMBO J 27:2147–2157.

11. Mansur DS, Maluquer de Motes C, Unterholzner L, Sumner RP, Ferguson BJ, Ren H, Strnadova P, Bowie AG, Smith GL. 2013. Poxvirus targeting of E3 ligase beta-TrCP by molecular mimicry: a mechanism to inhibit NF-kappaB activation and promote immune evasion and virulence. PLoS Pathog 9:e1003183.

12. Sumner RP, Maluquer de Motes C, Veyer DL, Smith GL. 2014. Vaccinia virus inhibits NF-kappaB-dependent gene expression downstream of p65 translocation. J Virol 88:3092–3102.

13. Wang Q, Burles K, Couturier B, Randall CM, Shisler J, Barry M. 2014. Ectromelia virus encodes a BTB/kelch protein, EVM150, that inhibits NF-kappaB signaling. J Virol 88:4853–4865.

14. Barry M, van Buuren N, Burles K, Mottet K, Wang Q, Teale A. 2010. Poxvirus exploitation of the ubiquitin-proteasome system. Viruses 2:2356–2380.

15. Shchelkunov SN. 2010. Interaction of orthopoxviruses with the cellular ubiquitin-ligase system. Virus Genes 41:309–318.

16. Pintard L, Willems A, Peter M. 2004. Cullin-based ubiquitin ligases: Cul3-BTB complexes join the family. EMBO J 23:1681–1687.

17. Ahmad KF, Engel CK, Prive GG. 1998. Crystal structure of the BTB domain from PLZF. Proc Natl Acad Sci U S A 95:12123–12128.

18. Adams J, Kelso R, Cooley L. 2000. The kelch repeat superfamily of proteins: propellers of cell function. Trends Cell Biol 10:17–24.

19. Ito N, Phillips SE, Yadav KD, Knowles PF. 1994. Crystal structure of a free radical

530 enzyme, galactose oxidase. J Mol Biol 238:794–814.

531 20. Mei ZZ, Chen XY, Hu SW, Wang N, Ou XL, Wang J, Luo HH, Liu J, Jiang Y. 2016.
532 Kelch-like Protein 21 (KLHL21) Targets IkB Kinase-B to Regulate Nuclear Factor
533 Kappa-Light Chain Enhancer of Activated B Cells (NF-kB) Signaling Negatively. J Biol
534 Chem 291:18176–18189.

535 21. Angers S, Thorpe CJ, Biechele TL, Goldenberg SJ, Zheng N, MacCoss MJ, Moon RT.
536 2006. The KLHL12-Cullin-3 ubiquitin ligase negatively regulates the Wnt-beta-catenin
537 pathway by targeting Dishevelled for degradation. Nat Cell Biol 8:348–357.

538 22. Yang Z, Bruno DP, Martens CA, Porcella SF, Moss B. 2010. Simultaneous high-
539 resolution analysis of vaccinia virus and host cell transcriptomes by deep RNA
540 sequencing. Proc Natl Acad Sci U S A 107:11513–11518.

541 23. Beard PM, Froggatt GC, Smith GL. 2006. Vaccinia virus kelch protein A55 is a 64 kDa
542 intracellular factor that affects virus-induced cytopathic effect and the outcome of
543 infection in a murine intradermal model. J Gen Virol 87:1521–1529.

544 24. Froggatt GC, Smith GL, Beard PM. 2007. Vaccinia virus gene F3L encodes an
545 intracellular protein that affects the innate immune response. J Gen Virol 88:1917–
546 1921.

547 25. Pires de Miranda M, Reading PC, Tscharke DC, Murphy BJ, Smith GL. 2003. The
548 vaccinia virus kelch-like protein C2L affects calcium-independent adhesion to the
549 extracellular matrix and inflammation in a murine intradermal model. J Gen Virol
550 84:2459–2471.

551 26. Stuart JH, Sumner RP, Lu Y, Snowden JS, Smith GL. 2016. Vaccinia Virus Protein C6
552 Inhibits Type I IFN Signalling in the Nucleus and Binds to the Transactivation Domain
553 of STAT2. PLoS Pathog 12:e1005955.

554 27. Winston JT, Strack P, Beer-Romero P, Chu CY, Elledge SJ, Harper JW. 1999. The

555 SCFbeta-TRCP-ubiquitin ligase complex associates specifically with phosphorylated
556 destruction motifs in IkappaBalpha and beta-catenin and stimulates IkappaBalpha
557 ubiquitination in vitro. Genes Dev 13:270–283.

558 28. Tscharke DC, Smith GL. 1999. A model for vaccinia virus pathogenesis and immunity
559 based on intradermal injection of mouse ear pinnae. J Gen Virol 80 (Pt 10):2751–
560 2755.

561 29. Tscharke DC, Reading PC, Smith GL. 2002. Dermal infection with vaccinia virus
562 reveals roles for virus proteins not seen using other inoculation routes. J Gen Virol
563 83:1977–1986.

564 30. Lauvau G, Boutet M, Williams TM, Chin SS, Chorro L. 2016. Memory CD8(+) T Cells:
565 Innate-Like Sensors and Orchestrators of Protection. Trends Immunol 37:375–385.

566 31. Shaw ML, Cardenas WB, Zamarin D, Palese P, Basler CF. 2005. Nuclear localization
567 of the Nipah virus W protein allows for inhibition of both virus- and toll-like receptor 3-
568 triggered signaling pathways. J Virol 79:6078–6088.

569 32. Ye J, Chen Z, Li Y, Zhao Z, He W, Zohaib A, Song Y, Deng C, Zhang B, Chen H, Cao
570 S. 2017. Japanese Encephalitis Virus NS5 Inhibits Type I Interferon (IFN) Production
571 by Blocking the Nuclear Translocation of IFN Regulatory Factor 3 and NF-kappaB. J
572 Virol 91:e00039-17.

573 33. Gagne B, Tremblay N, Park AY, Baril M, Lamarre D. 2017. Importin beta1 targeting by
574 hepatitis C virus NS3/4A protein restricts IRF3 and NF-kappaB signaling of IFNB1
575 antiviral response. Traffic 18:362–377.

576 34. Taylor SL, Frias-Staheli N, Garcia-Sastre A, Schmaljohn CS. 2009. Hantaan virus
577 nucleocapsid protein binds to importin alpha proteins and inhibits tumor necrosis
578 factor alpha-induced activation of nuclear factor kappa B. J Virol 83:1271–1279.

579 35. Gao C, Pallett MA, Croll, TI, Smith, GL Graham, SC. Molecular basis of Cul3 ubiquitin

ligase subversion by vaccinia virus protein A55. J Biol Chem, under revision.

36. Huotari J, Meyer-Schaller N, Hubner M, Stauffer S, Katheder N, Horvath P, Mancini R, Helenius A, Peter M. 2012. Cullin-3 regulates late endosome maturation. Proc Natl Acad Sci U S A 109:823–828.

37. Kaech SM, Cui W. 2012. Transcriptional control of effector and memory CD8(+) T cell differentiation. Nat Rev Immunol 12:749–761.

38. Ren H, Ferguson BJ, Maluquer de Motes C, Sumner RP, Harman LER, Smith GL. 2015. Enhancement of CD8(+) T-cell memory by removal of a vaccinia virus nuclear factor-kappaB inhibitor. Immunology 145:34–49.

39. Unterholzner L, Sumner RP, Baran M, Ren H, Mansur DS, Bourke NM, Randow F, Smith GL, Bowie AG. 2011. Vaccinia Virus Protein C6 Is a Virulence Factor that Binds TBK-1 Adaptor Proteins and Inhibits Activation of IRF3 and IRF7. PLoS Pathog 7:e1002247.

40. Pallett MA, Berger CN, Pearson JS, Hartland EL, Frankel G. 2014. The type III secretion effector NleF of enteropathogenic Escherichia coli activates NF-kappaB early during infection. Infect Immun 82:4878–4888.

41. Parkinson JE, Smith GL. 1994. Vaccinia virus gene A36R encodes a M(r) 43-50 K protein on the surface of extracellular enveloped virus. Virology 204:376–390.

42. Everett RD, Bell AJ, Lu Y, Orr A. 2013. The replication defect of ICP0-null mutant herpes simplex virus 1 can be largely complemented by the combined activities of human cytomegalovirus proteins IE1 and pp71. J Virol 87:978–990.

Figure Legends

Fig. 1. A55 inhibits NF-κB dependent signalling. (A, B) HEK293T cells were transfected with pLuc-NF-κB and pRL-TK (Methods) and plasmids expressing Flag-tagged KLHL12, B14 or A55 or empty vector (EV). After 24 h cells were stimulated with (A) 15 ng/ml IL-1β or (B) 20 ng/ml TNFα for 6 h. Cell lysates were prepared and the fold increase in luciferase activity relative to Renilla activity was determined. In parallel, cell lysates were analysed by SDS-PAGE and immunoblotting with anti-Flag or anti-α-tubulin to determine protein expression levels from unstimulated samples. Data are representative of three independent experiments. Statistical significance compares EV stimulated with test sample. (C). As in (A) using increasing plasmid concentration of pCNDA4/TO-nTAP A55 at 25, 75 and 150 ng. Statistical significance compares EV stimulated with A55 stimulated. (D). HEK293T pCW57 stable cell lines inducibly expressing C6, B14 or A55 were induced with 2 µg/ml doxycycline for 24 h, starved for 6 h in DMEM with no supplements and left unstimulated, or stimulated with TNFA for 18 h. Levels of secreted CXCL10 in the cell culture medium were assayed by ELISA. Data shown are representative of 2 independent experiments carried out in triplicate. Statistical significance compares C6 stimulated with B14 or A55. (E) T-REx cell lines inducibly expressing B14 or A55 were induced with 2 µg/ml doxycycline for 22.5 h and left unstimulated or stimulated with 20 ng/ml TNFA for 1.5 h in DMEM with no supplements. *IL-8* expression levels were analysed by RT-qPCR relative to *GAPDH*. Data presented are representative of 2 independent experiments carried out in triplicate. Statistical significance, C6 stimulated vs A55 stimulated. (F, G). A55 does not inhibit MAPK or JAK-STAT signalling. HEK293T cells were transfected with (F) pAP-1-Luc or (G) pISRE-Luc and pRL-TK (Methods) and plasmids ex-pressing Flag-tagged KLHL12, C6 or A55 or

627 empty vector (EV). After 24 h cells were stimulated with (F) 10 ng/ml PMA or (G)
628 1000 U/ml IFNα for 6 h. Cell lysates were prepared and the fold increase in
629 luciferase activity relative to Renilla activity was determined. In parallel, cell lysates
630 were analysed by SDS-PAGE and immunoblotting with anti-Flag or anti-α-tubulin to
631 determine protein expression levels from unstimulated samples. Data are
632 representative of three independent experiments. Statistical significance compares
633 EV stimulated with test sample.

Fig. 2. A55 inhibits NF-κB activation downstream of p65 release. HEK293T cells were transfected with pLuc-NF-κB and pRL-TK together with plasmids expressing Flag-tagged KLHL12, B14 or A55 or EV and either (A) TRAF6, (B) TRAF2, (C) TAK1, or (D) IKKβ. After 24 h the fold difference in luciferase activity was determined and the abundance of indicated proteins was measured by SDS-PAGE and immunoblotting. (E) Cells were transfected with reporters as above together with a Flag-tagged p65 expression plasmid and increasing doses of plasmid expressing A55 (25, 75, 150 ng). Experiments are representative of 3 independent experiments carried out in quadruplicate. Statistical significance compares EV stimulated with test sample stimulated.

643 Fig. 3. A55 acts downstream of IκBα degradation and prevents phosphorylation of p65 on
644 Ser276. HEK293T-REx cell lines inducibly expressing B14, or A55, or empty vector (EV)
645 were induced with 2 μg/ml doxycycline for 24 h and then stimulated with 40 ng/ml TNFα for
646 20 min. The levels of IκBα, Flag-tagged B14 or A55, and α-tubulin were determined by SDS-
647 PAGE and immunoblotting. (B) The level of IκBα relative to tubulin was quantified by
648 densitometry from 3 independent experiments. Statistical significance compares EV
649 stimulated with B14 or A55 stimulated conditions. (C). HEK293T-REx cell lines inducibly
650 expressing A55 or EV were induced with doxycline as in (A) and then left unstimulated (0) or
651 stimulated with 40 ng/ml TNFα for 30 or 60 min. The levels of indicated proteins and
652 phosphorylation of p65 were determined by SDS-PAGE and immunoblotting. Loading and
653 p65 levels were controlled for using anti-tubulin and anti-p65, respectively. The immunoblot
654 shown is representative of 3 independent experiments.

Fig. 4 A55 inhibits p65 nuclear translocation. (A) Representative immunofluorescent staining of p65 localisation in HeLa cells transfected with 1000 ng / well of a 6-well plate of plasmids encoding Flag-tagged B14, A55, C6 or EV and left untreated or stimulated with 20 ng/ml TNFα for 30 min. Cells were stained with DAPI (blue), anti-Flag (red) and anti-p65 (green) antibodies. (B) Percentage of transfected cells with nuclear p65. Representative of 3 independent experiments, carried out in triplicate, counting 100 cells per sample. Statistical significance compares EV stimulated with A55, B14, or C6 stimulated. Scale bars, 10 μM.

Fig. 5. A55 targets host importin KPNA2. (A-C) Representative immunoblots showing (A-B) anti-Flag, or (C) anti-HA immunoprecipitation (IP) of cleared lysates from HEK293T cells lysed in (A-B) NP40 or RIPA (C) buffer and subjected to SDS-PAGE and immunoblotting with stated antibodies. (A) HEK293T cells were transfected with plasmids encoding Flag-KPNA1, KPNA2, KPNA3 or EV and 24 h later cells were infected with WT VACV at 5 p.f.u./cell for 18 h. (B) HEK293T-REx cells inducibly expressing B14, A55 or EV were induced with 2 µg/ml doxycline for 36 h. (C) pCW57 cell lines expressing B14 or A55 inducibly were induced with 2 µg/ml doxycycline for 24 h and then transfected with a plasmid encoding HA-tagged p65. Input, cleared cell lysate; IP, immunoprecipitate. IB, immunoblot. In the right panel, the amount of KPNA2 co-precipitating with p65 in the presence of A55 or B14 was quantified by densitometry. Average of 3 independent experiments. (D) Endogenous KPNA2 levels in cell lysates from HeLa cells infected for 3, 6, or 9 h with vA55, vΔA55 or vΔA55Rev at 5 p.f.u/cell or left non-infected (NI). Tubulin was used as a loading control and VACV protein D8 as a control for infection. The immunoblot shown is representative of 2 independent experiments.

Fig. 6. A55 inhibits NF-κB activation in a cullin-3-independent manner via its Kelch domain. (A) Immunoblots following immunoprecipitation (IP) of cleared cell lysates from HEK293T-REx cells inducibly expressing (A) B14, A55 or EV, (B) B14 or A55, (C) B14, A55, A55-BTB, A55-Kelch, or EV, 24 h post induction with 2 μg/ml doxycycline and lysis in NP40 (A and D) or RIPA (B) lysis buffer. Samples were subjected to SDS-PAGE and immunoblotting with the stated antibodies. (A and D) Flag-tagged immunoprecipitation and immunoblotting for endogenous cullin-3. (B) Reciprocal IP with protein G-Sepharose supplemented with mouse anti-Myc using cell lysates prepared 24 h post-transfection with pCDNA-Myc-*CUL3* or *CUL5*. (C) Schematic of A55 domains. Full length A55 from amino acid 1 to 565 was divided into the N-terminal BTB-BACK containing domain and the C-terminal Kelch domain as depicted. (E) Flag IP as with (D) in RIPA buffer using the pCW57 HEK cell lines expressing B14, A55, A55-BTB or A55-Kelch and blotting for endogenous KPNA2. Input, cleared lysate; IP, immunoprecipitate; IB, immunoblot. *, antibody heavy/light chain. (F) HEK293T cells were transfected with pLuc-NF-κB and pRL-TK together with 100 ng pcDNA3-Flag-*KLHL12*, 20 ng pcDNA4-*coB14R*-Flag, 100 ng pcDNA4/TO-nTAP-*coA55R*, pcDNA4/TO-nTAP-*coA55R*-BTB, pcDNA4/TO-nTAP-*coA55R*-Kelch or pcDNA4/TO-EV. In the right panel cells were also transfected with plasmid expressing TRAF6. After 24 h cells were either left unstimulated or stimulated with 15 ng/ml IL-1β for 6 h and the luciferase and renilla activity were measured. Statistical significance compared EV (stimulated) with test samples. (G). Lysates from cells treated (as in F, left panel) were analysed by SDS-PAGE and immunoblotting with the indicated antibodies. Data shown in all panels are representative of 3 independent experiments.

Fig. 7. The A5 Kelch domain inhibits p65 nuclear translocation. (A) Representative immunofluorescent staining of p65 localisation in HeLa cells transfected with plasmids encoding Flag-tagged B14, A55, C6 or EV and left untreated or stimulated with 40 ng/ml TNFα for 30 min. Cells were stained as described in Methods with DAPI (blue), anti-Flag (red) and anti-p65 (green). Scale bars, 20 μM. (B) Percentage of transfected cells with nuclear p65. Representative of 3 independent experiments. Statistical significance compares EV (stimulated) with A55, B14, or C6 (stimulated). (C) Representative image of HeLa cells transfected with a plasmid encoding A55-BTB. Scale bar, 10 μM. Representative of 3 independent experiments.

Fig. 8. Infection with vΔA55 induces enhanced $CD8^+$ T-cell response. Female C57/Bl6 mice (6-8 weeks old, n=5) were injected intradermally in the ear pinnae with 5 x 10^3 p.f.u. of purified vA55, vΔA55 or vΔA55Rev, or PBS. At 7 d p.i. the total number of cells in (A) spleen and (B) draining lymph node (DLN) were determined. The absolute number of $CD8^+$ or $CD4^+$ T-cells from spleen (A) or DLN (B), and the number of splenic NK cells, macrophages, and neutrophils (A) were determined by FACs. The expression of CD69 on (C) splenic NK, $CD4^+$ and $CD8^+$ cells and on (D) DLN $CD4^+$ and $CD8^+$ cells was quantified. (E) Number of splenic, VACV-specific, DimerX positive $CD8^+$ T cells at day 7 and 28 p.i. Statistical analysis compares vΔA55 with vA55 or vA55Rev. Data shown are representative of 2 independent experiments.

718 Fig. 9. Infection with vΔA55 induces enhanced $CD8^+$ T cell cytotoxicity and better protection
719 to VACV challenge. Mice were infected as in Fig. 7 and the immune response was analysed
720 at 28 d p.i. (A) ^{51}Cr-release assay assessing the ability of splenic $CD8^+$ T cells to lyse VACV-
721 infected EL4 cells, or splenic NK cells to lyse VACV-infected P815 cells. Data are presented
722 as percentage cell lysis at various effector to target (E:T) cell ratios. (B) ^{51}Cr-release assay
723 conducted as in (A) but pre-incubated with a monoclonal anti-CD8 antibody. (C and D). At 28
724 d p.i. with vA55, vΔA55 or vΔA55Rev immunised mice were infected with 10^7 p.f.u. of WT
725 VACV and the weight change (C) and pulmonary virus titres (D) were determined. Statistical
726 analysis compares vΔA55 with vA55 or vA55Rev. Data shown are representative of 2
727 independent experiments.

728

729 **Table 1. Plasmids constructed or used in this study**

Parental plasmid	Description		Reference/Source
pcDNA4/TO-nTAP/nHA/cTAP	Mammalian expression vector with N-terminal or C-terminal STREPI and STREPII tag followed by Flag tag or with a C-terminal HA tag only or a C-terminal Flag tag only, all under the control of a CMV promoter, Amp^r, Zeo^r		Invitrogen
	Primer	**RE**	
pcDNA4/TO-nTAP-*A55R*	GACGCGGCCGCGAACAACAGCAGCGAGC GACTCTAGATCAGCTTCCGATGAAGC	NotI XbaI	This study
pcDNA4/TO-nTAP-*A55R* BTB	GACGCGGCCGCGAACAACAGCAGCGAGC GACTCTAGATTAGTGGTATCTGGGGAAGC	NotI XbaI	This study
pcDNA4/TO-nTAP-*A55R* Kelch	GACGCGGCCGCGTCCATCGAGCTGATCAGC GACTCTAGATCAGCTTCCGATGAAGC	NotI XbaI	This study
pcDNA4/TO-*P65*-cTAP	ATATCGGATCCGCCACCATGGACGAACTGTTCCCCCTCATCT ATACTGCGGCCGCGGAGCTGATCTGACTCAGC	BamHI NotI	This study
pcDNA4/TO-*P65*-HA	ATATCGCGGCCGCGGACGAACTGTTCCCCCTCATCT ATACTTCTAGATTAGGAGCTGATCTGACTCAGC	NotI XbaI	This study
pCDNA4/TO-*B14R*-cTAP	GCGCGGATCCACCATGACGGCCAACTTTAGTACCCACGTC GCTGCCTCCTCCCTTTTCAAACTGAGGATGAGACCACGCGG CCGCATTCATACGCCGGAATATG GCCGCTGGCTCCCTTCTCGAACTGGGGGTGGCTCCAGCTTC CGCCTCCGCTGCCTCCTCCCTT CGGCTCTAGACCGCGGTTACTTGTCGTCATCGTCATCCTTGT AGTCCTCGCCGCTGGCTCCCTTCTC	BamHI XbaI	This study
pCDNA™6/TR	Mammalian expression vector with the Tet Repressor under the control of a CMV promoter, Amp^r, Blast^r		Invitrogen
pCDNA3-Flag/HA/Myc	Mammalian expression vector with Flag or HA tag under the control of a CMV promoter, Amp^r		Invitrogen
	Primer	**RE**	
pcDNA3-HA-*TAK1*	GCTGCGGCCGCTTCTACAGCCTCTGCC GTCTCTAGATCATGAAGTGCCTTGTCG	NotI XbaI	This study
pcDNA3-HA-*TAB1*	GCTGCGGCCGCATGGCGGCGCAGAGGAGGAGC GTCTCTAGACTACGGTGCTGTCACCACGCT	NotI XbaI	This study
pcDNA3-Flag-*KLHL12*	N/A	N/A	Gift, Randall T Moon
pcDNA3-Flag-*CUL3*	N/A	N/A	Addgene, 19893
pcDNA3-Flag-*CUL5*	N/A	N/A	Addgene, 19895
M5P-Flag	Mammalian expression vector with Flag tag under the control of the Murine Leukaemia virus (MLV) LTR promoter, Amp^r		
M5P-Flag-*TRAF6*	N/A	N/A	Gift, Andrew Bowie
pCW57-GFP-P2A-MCS	Lentiviral expression plasmid with GFP in MSC1 and P2A skip sequence followed by MCS2 under the control of a CMV promoter, Amp^r and Puro^r		Addgene, 89181
	Primer	**RE**	
pCW57-GFP-P2A-nTAP-*A55R*	CGACGCGTATGTGGTCTCATCCTCAGTTTG GCAGGATCCTCAGCTTCCGATGAAGCTTTC	MluI BamHI	This study
pCW57-GFP-P2A-nTAP-*A55R* BTB	CGACGCGTATGTGGTCTCATCCTCAGTTTG GCAGGATCCTCAGTGGTATCTGGGGAAGC	MluI BamHI	This study
pCW57-GFP-P2A-nTAP-*A55R* Kelch	CGACGCGTATGTGGTCTCATCCTCAGTTTG GCAGGATCCTCAGCTTCCGATGAAGCTTTC	MluI BamHI	This study
pCW57-GFP-P2A-nTAP-*B14R*	CGACGCGTATGTGGTCTCATCCTCAGTTTG GCAGGATCCTCAATTCATACGCCGGAATAT	MluI BamHI	This study
pCW57-GFP-P2A-nTAP-*C6L*	CGACGCGTATGTGGTCTCATCCTCAGTTTG CGACGCGTTTATCATCTGTCCACGTCGT	MluI MluI	This study
pCMV-PACK	Packaging plasmid for lentivirus production with HIV Gag, Pol, Rev and Tat under the CMV promotor, Amp^r		Gift, Dr. H. Laman
pCMV-ENV	VSV-G pseudotyped envelope protein under the CMV promoter for lentivirus production, Amp^r		Gift, Dr. H. Laman

pLDT-TetR	Lentiviral expression plasmid constitutively expressing the Tetracyline promoter repressor, Amp^r and Neo^r		(42)
pLDT-MCS	Lentiviral expression plasmid with expression under the control of a Tetracycline inducible CMV promoter, Amp^r and Puro^r		(42)
	Primer	**RE**	
pLDT-nTAP-*A55R*	CTAGCTAGCATGTGGTCTCATCCTCAGTTTG GCGGTCGACTCAGCTTCCGATGAAGCTTTC	NheI SalI	This study
pLDT-nTAP-*B14R*	CTAGCTAGC ATGTGGTCTCATCCTCAGTTTG CGGAATTCTCAATTCATACGCCGGAATAT	NheI EcoRI	This study
pLDT-nTAP-*C6L*	CTAGCTAGCATGTGGTCTCATCCTCAGTTTG GAGCTCGAATTCTTATCATCTGTCCACGTCGT	NheI EcoRI	This study
pCAGGS-Flag	Mammalian expression vector with Flag tag under the control of the CMV-IE promoter, Amp^r		
	Primer	**RE**	
pCAGGS-Flag-KPNA1	N/A	N/A	(31)
pCAGGS-Flag-KPNA2	N/A	N/A	(31)
pCAGGS-Flag-KPNA3	N/A	N/A	(31)

Amp^r, Ampicillin resistance; Puro^r, Puromycin resistance; Neo^r, Neomycin resistance; Zeo^r, Zeocin resistance; Blast^r, Blasticidin resistance.

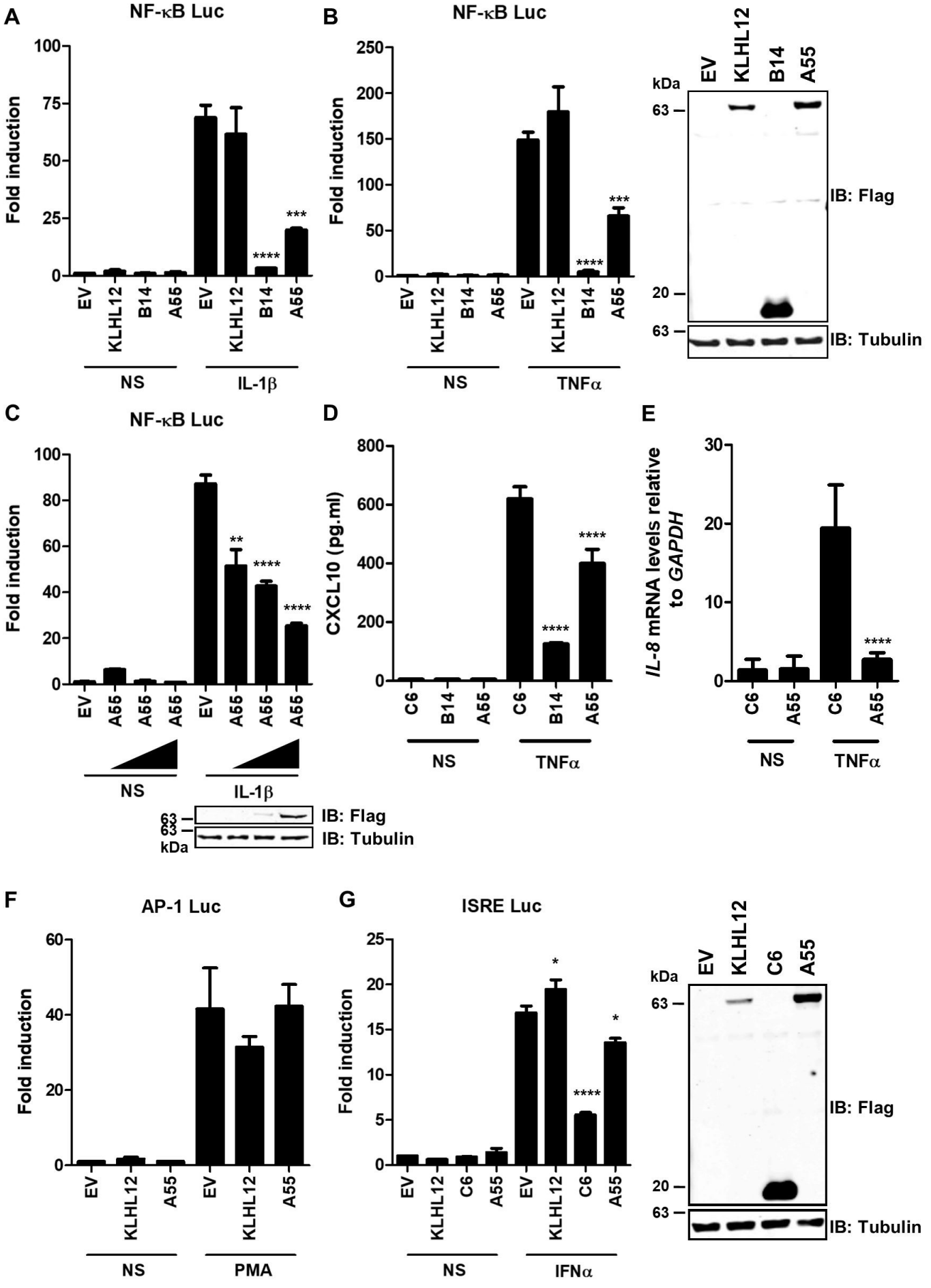
A
NF-κB Luc
Fold induction
EV
KLHL12
B14
A55
NS
IL-1β
B
NF-κB Luc
TNFα
kDa
63
20
IB: Flag
IB: Tubulin
C
NF-κB Luc
D
CXCL10 (pg.ml)
C6
E
IL-8 mRNA levels relative to GAPDH
F
AP-1 Luc
PMA
G
ISRE Luc
IFNα

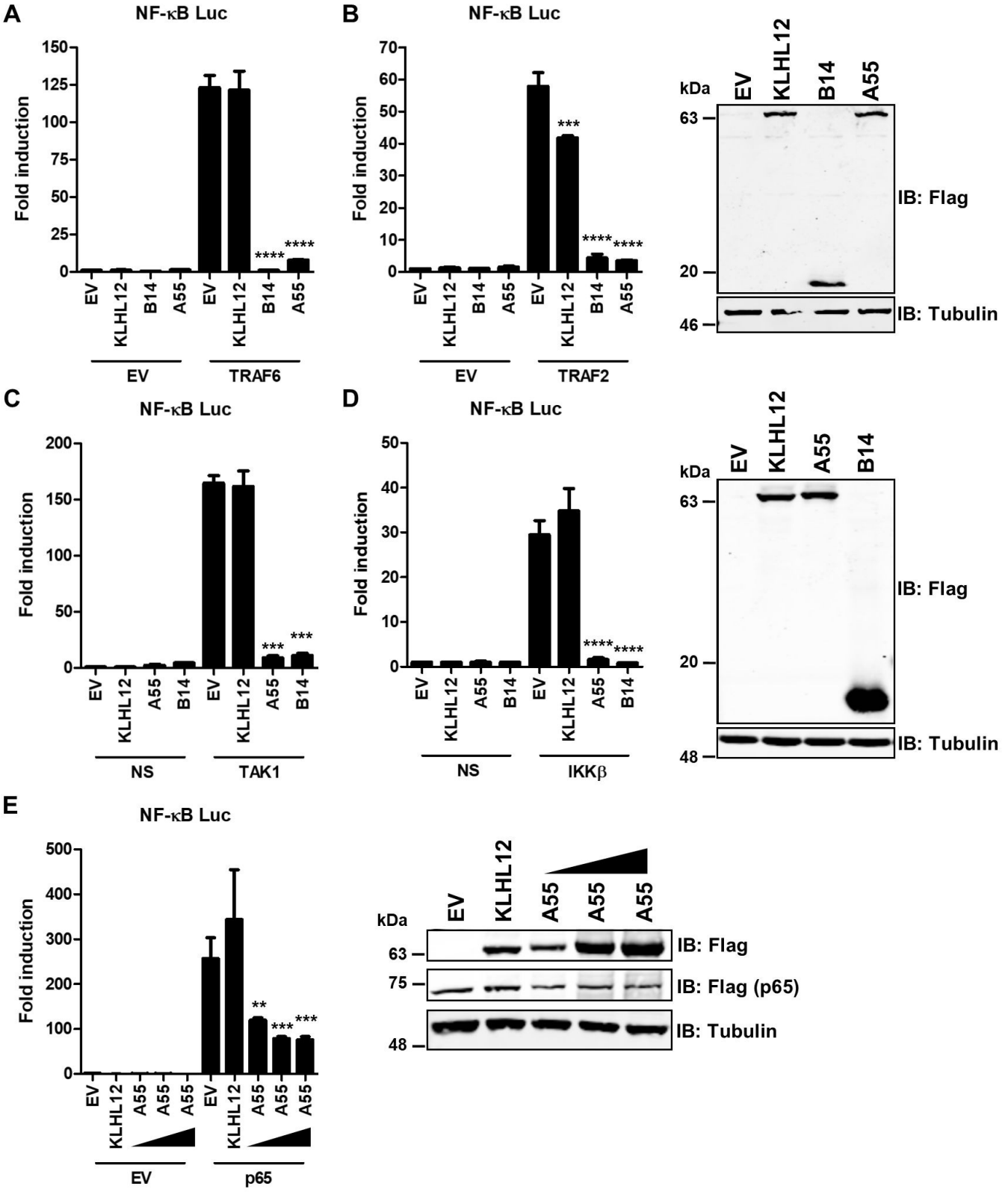
A
NF-κB Luc
Fold induction
150
125
100
75
50
25
0
EV
KLHL12
B14
A55
EV
KLHL12
B14
A55
****
****
EV
TRAF6
B
NF-κB Luc
Fold induction
70
60
50
40
30
20
10
0
***
****
****
EV
TRAF2
kDa
EV
KLHL12
B14
A55
63
20
46
IB: Flag
IB: Tubulin
C
NF-κB Luc
Fold induction
200
150
100
50
0
***
***
NS
TAK1
D
NF-κB Luc
Fold induction
50
40
30
20
10
0
****
****
NS
IKKβ
kDa
EV
KLHL12
A55
B14
63
20
48
IB: Flag
IB: Tubulin
E
NF-κB Luc
Fold induction
500
400
300
200
100
0
**
***
***
EV
p65
kDa
EV
KLHL12
A55
A55
A55
63
75
48
IB: Flag
IB: Flag (p65)
IB: Tubulin

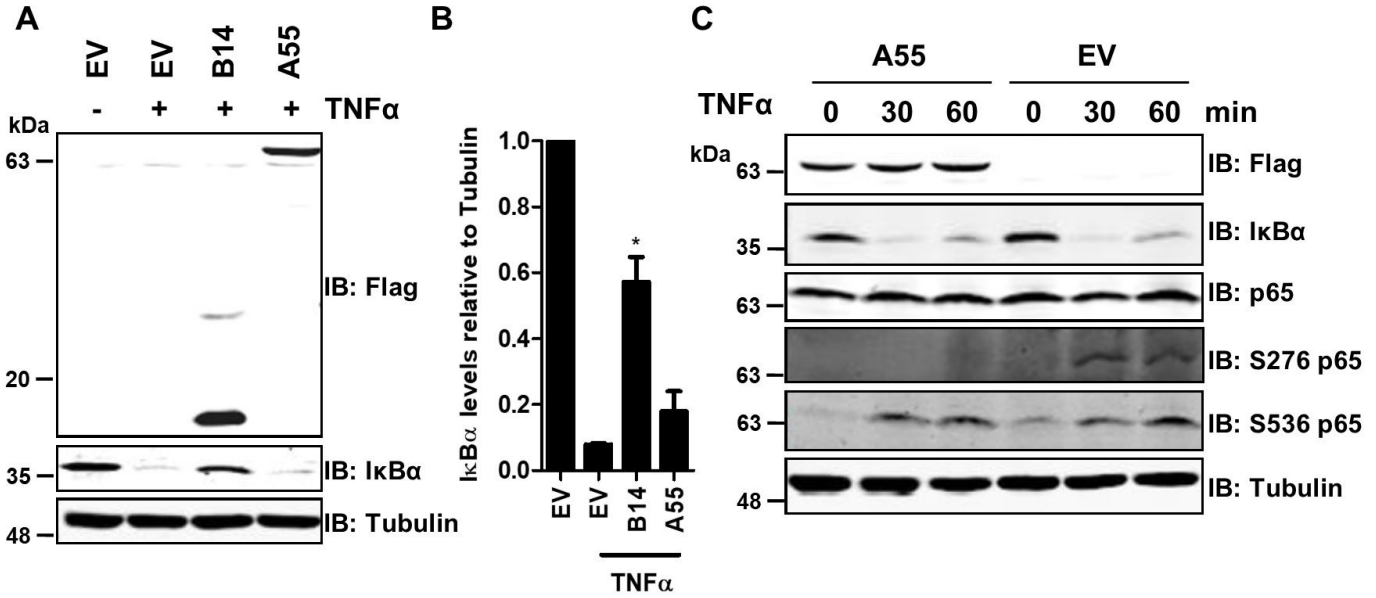
A
EV
EV
B14
A55
-
+
+
+
TNFα
kDa
63
20
35
48
IB: Flag
IB: IκBα
IB: Tubulin
B
IκBα levels relative to Tubulin
1.0
0.8
0.6
0.4
0.2
0.0
*
EV
EV
B14
A55
TNFα
C
A55
EV
TNFα
0
30
60
0
30
60
min
kDa
63
35
63
63
63
48
IB: Flag
IB: IκBα
IB: p65
IB: S276 p65
IB: S536 p65
IB: Tubulin

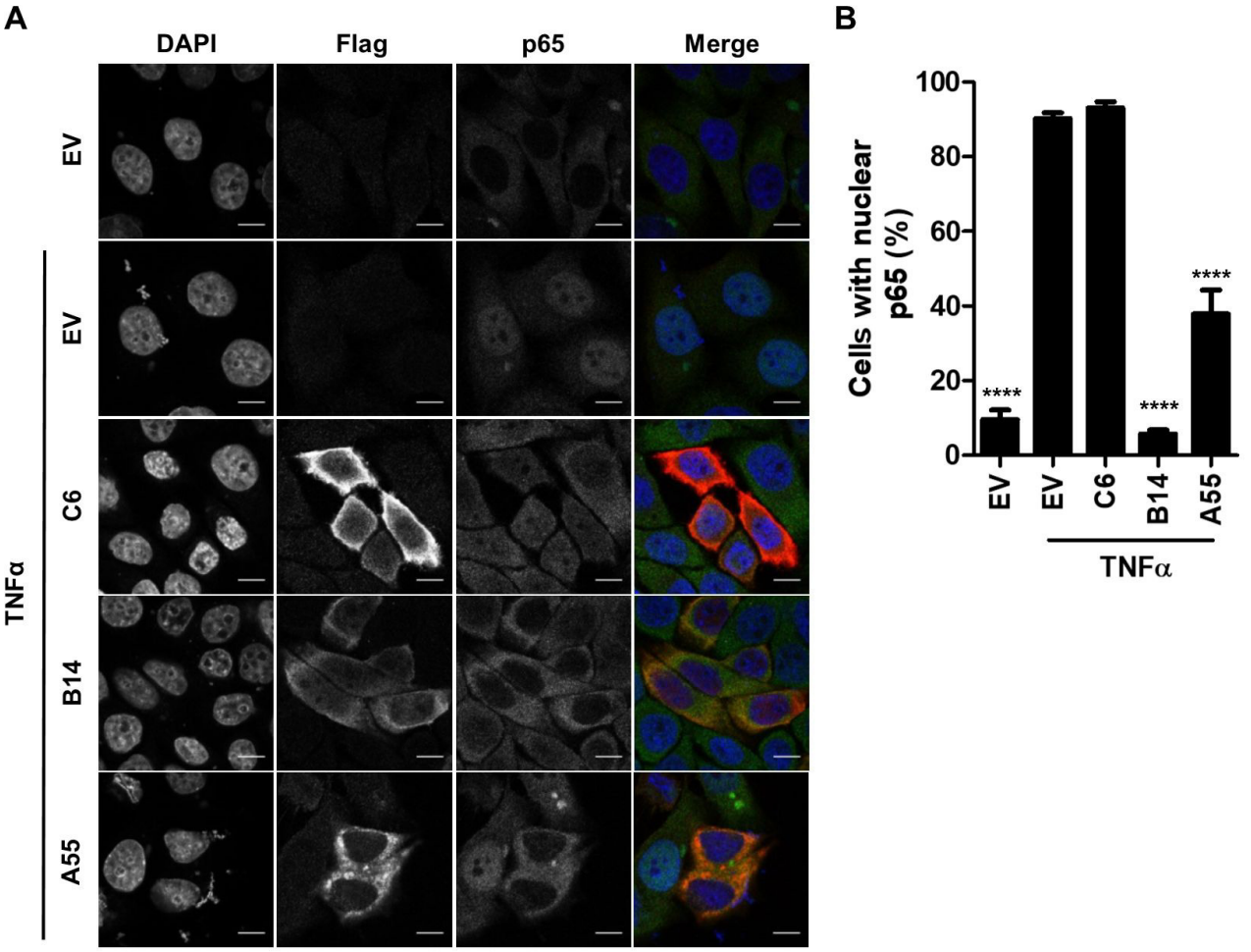
A
DAPI
Flag
p65
Merge
EV
EV
C6
B14
A55
TNFα
B
Cells with nuclear p65 (%)
100
80
60
40
20
0
****
****
****
EV
EV
C6
B14
A55
TNFα

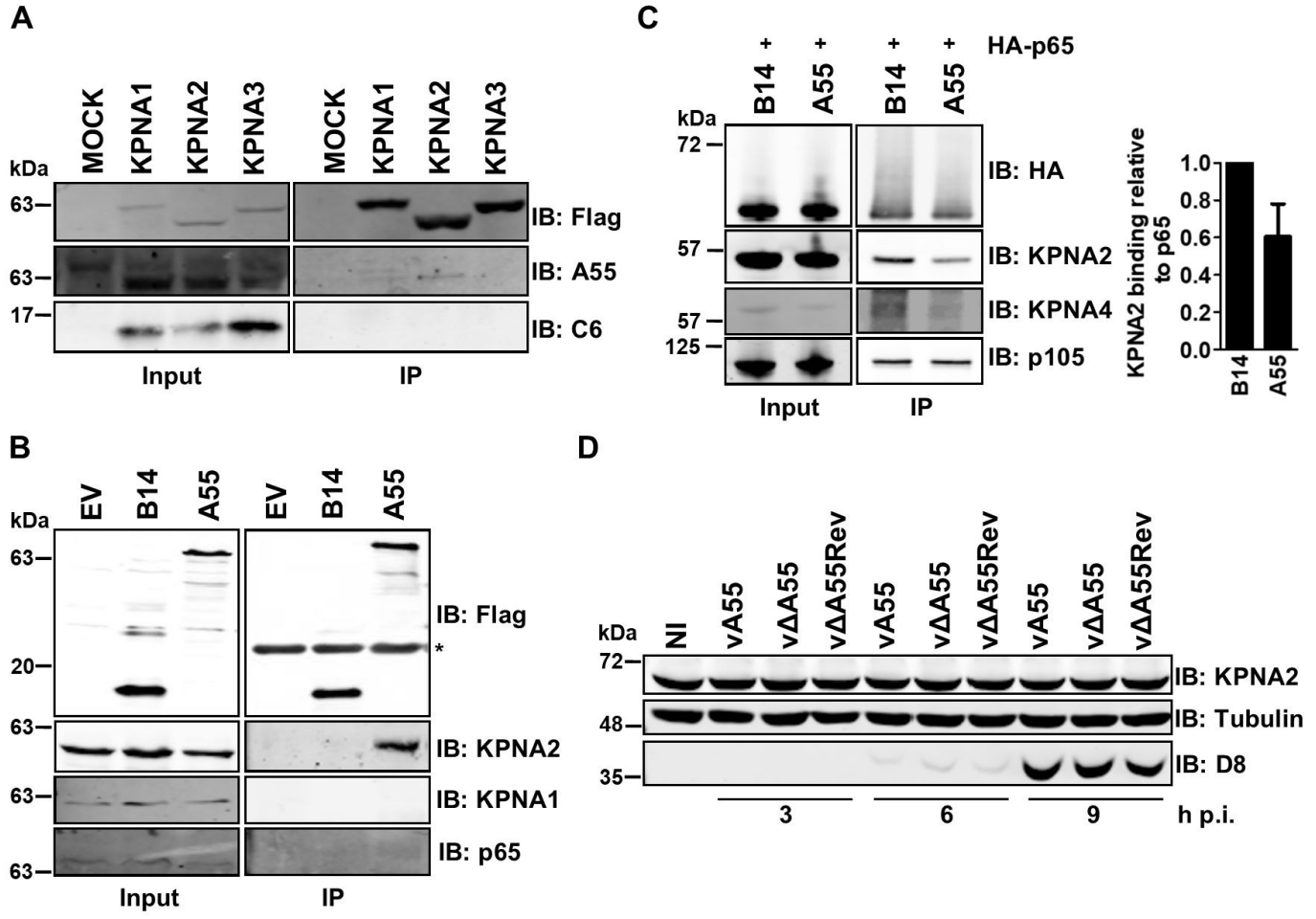
A
MOCK
KPNA1
KPNA2
KPNA3
MOCK
KPNA1
KPNA2
KPNA3
kDa
63
63
17
IB: Flag
IB: A55
IB: C6
Input
IP
B
EV
B14
A55
EV
B14
A55
kDa
63
20
63
63
63
IB: Flag
*
IB: KPNA2
IB: KPNA1
IB: p65
Input
IP
C
HA-p65
B14 +
A55 +
B14 +
A55 +
kDa
72
57
57
125
IB: HA
IB: KPNA2
IB: KPNA4
IB: p105
Input
IP
KPNA2 binding relative to p65
1.0
0.8
0.6
0.4
0.2
0.0
B14
A55
D
NI
vA55
vΔA55
vΔA55Rev
vA55
vΔA55
vΔA55Rev
vA55
vΔA55
vΔA55Rev
kDa
72
48
35
IB: KPNA2
IB: Tubulin
IB: D8
3
6
9
h p.i.

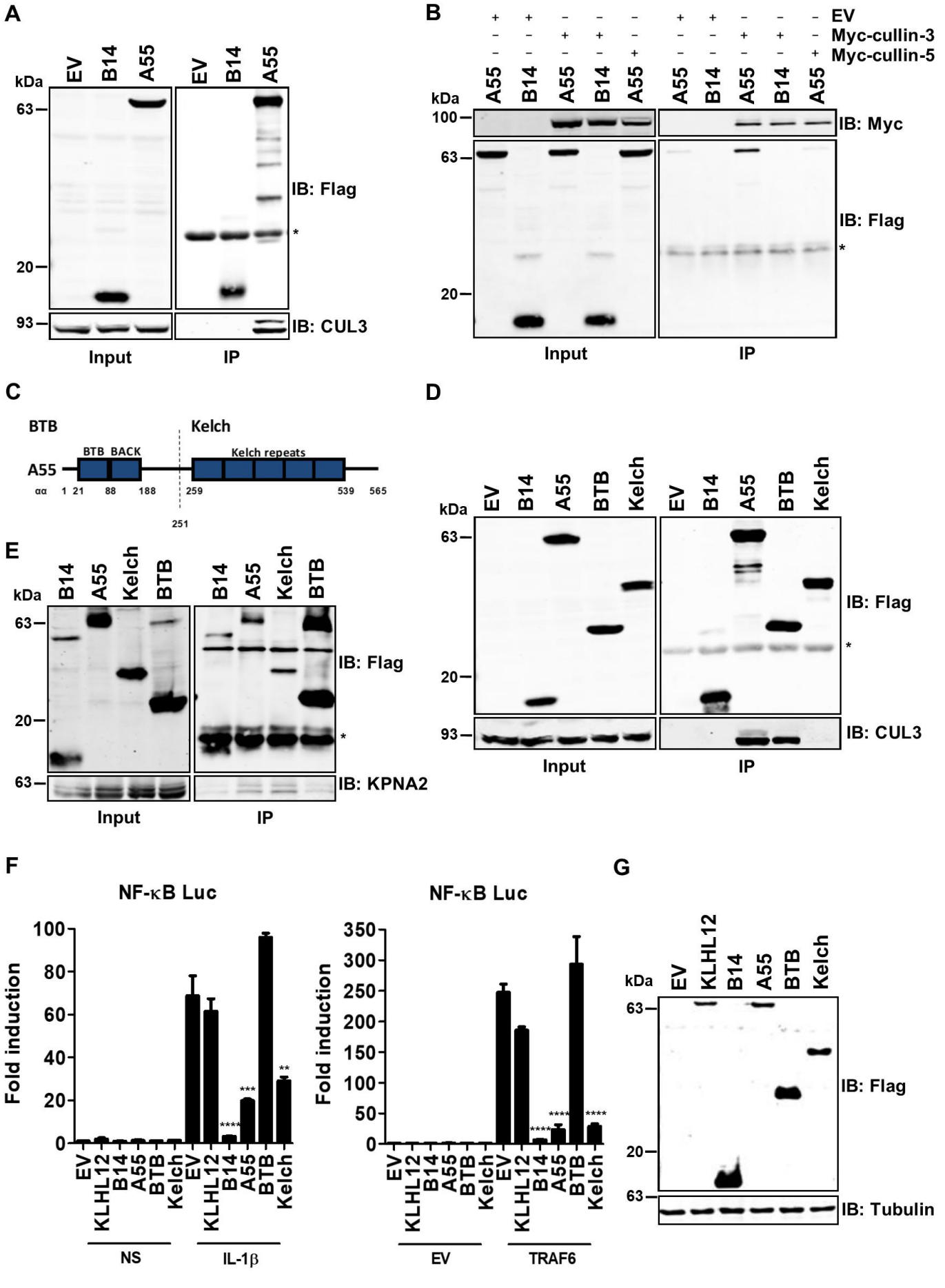
A
kDa
EV
B14
A55
63
20
93
IB: Flag
IB: CUL3
Input
IP
B
EV
Myc-cullin-3
Myc-cullin-5
100
IB: Myc
IB: Flag
C
BTB
Kelch
BTB BACK
Kelch repeats
A55
αα 1 21 88 188 259 539 565
251
D
BTB
E
IB: KPNA2
F
NF-κB Luc
Fold induction
KLHL12
NS
IL-1β
TRAF6
G
IB: Tubulin

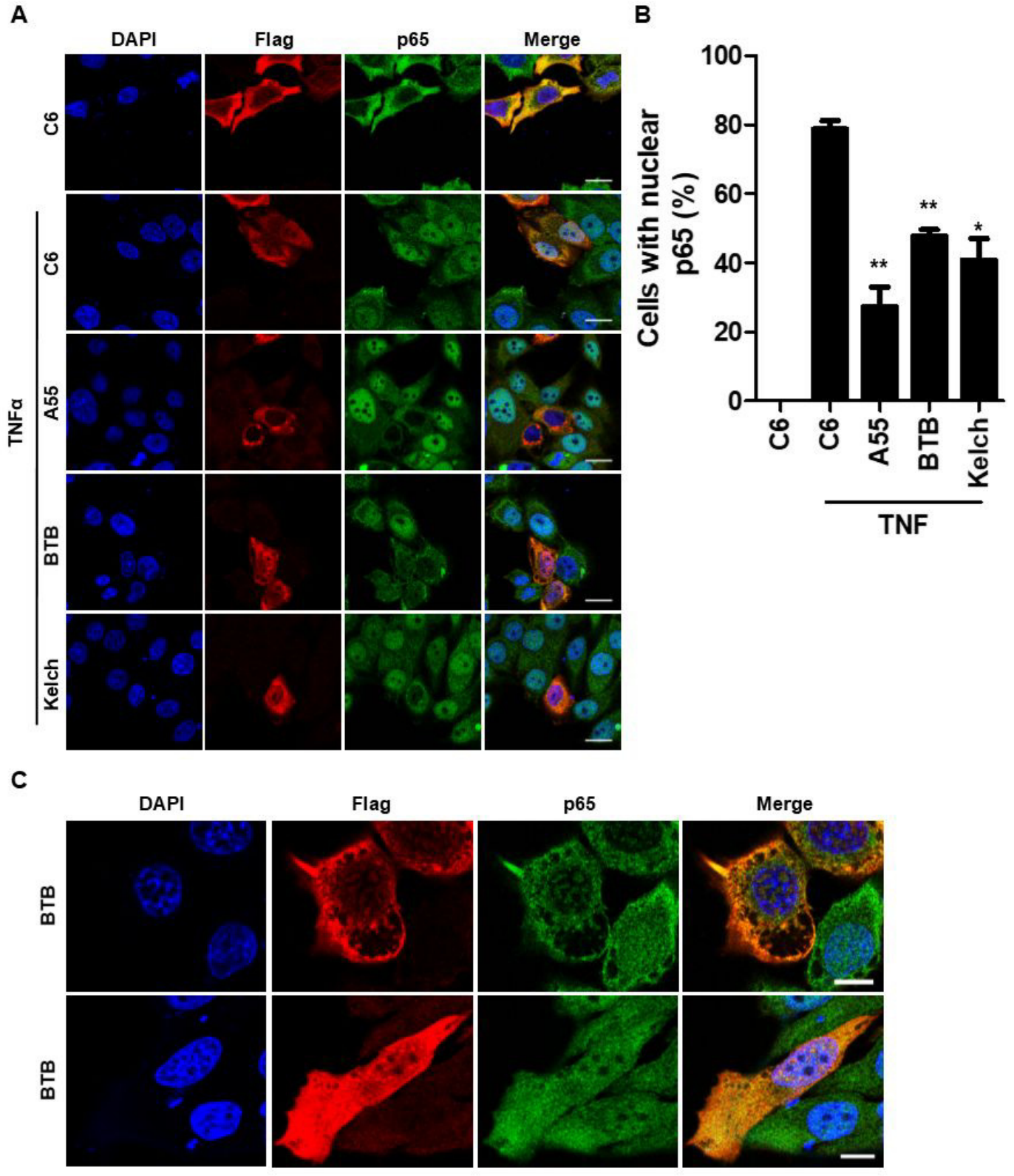
A
DAPI
Flag
p65
Merge
C6
TNFα
C6
A55
BTB
Kelch
B
Cells with nuclear p65 (%)
100
80
60
40
20
0
**
**
*
C6
C6
A55
BTB
Kelch
TNF
C
DAPI
Flag
p65
Merge
BTB
BTB

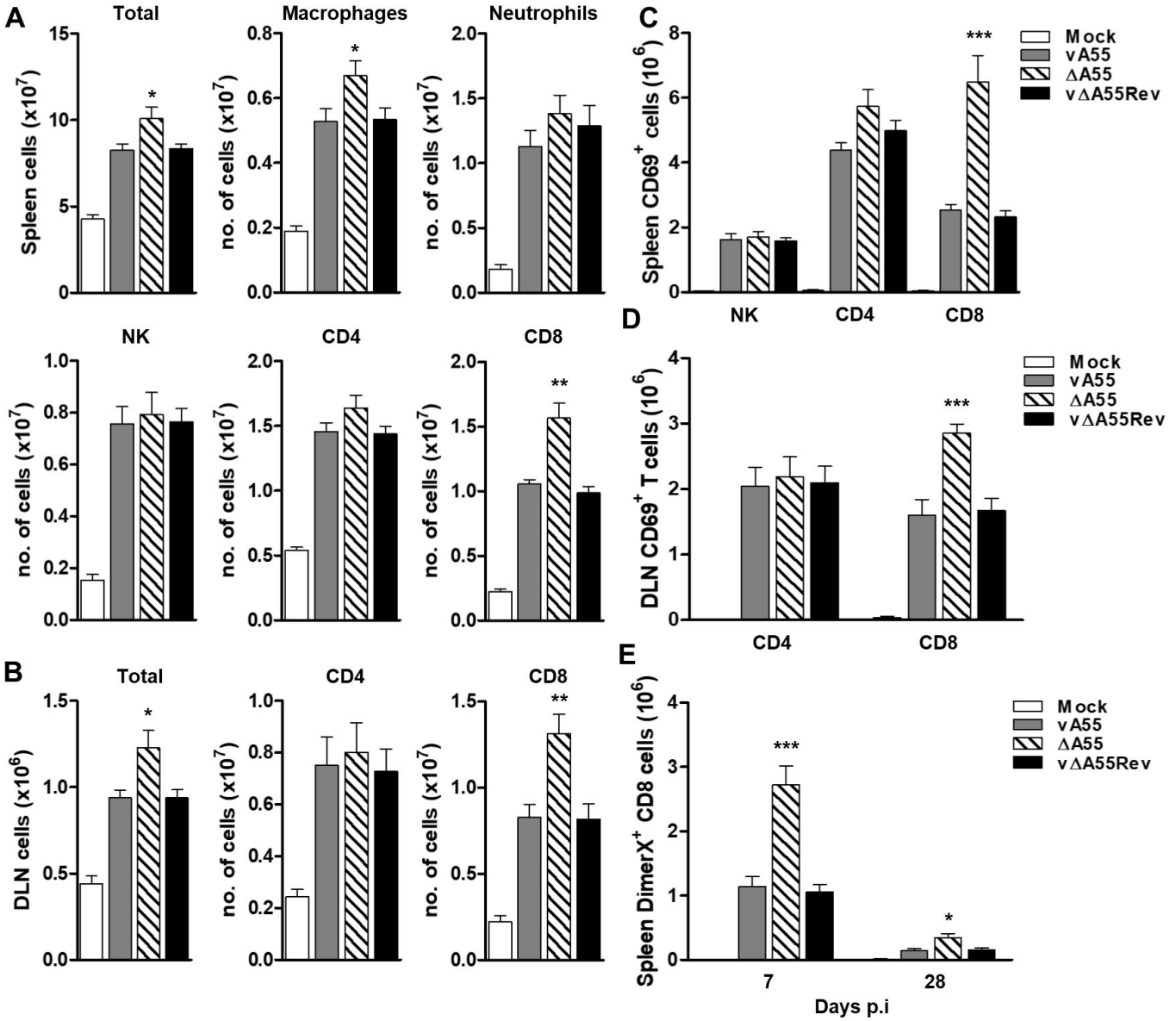
A
Total
Macrophages
Neutrophils
Spleen cells (x10^7)
no. of cells (x10^7)
NK
CD4
CD8
B
DLN cells (x10^6)
C
Spleen CD69+ cells (10^6)
D
DLN CD69+ T cells (10^6)
E
Spleen DimerX+ CD8 cells (10^6)
7
28
Days p.i
Mock
vA55
ΔA55
vΔA55Rev

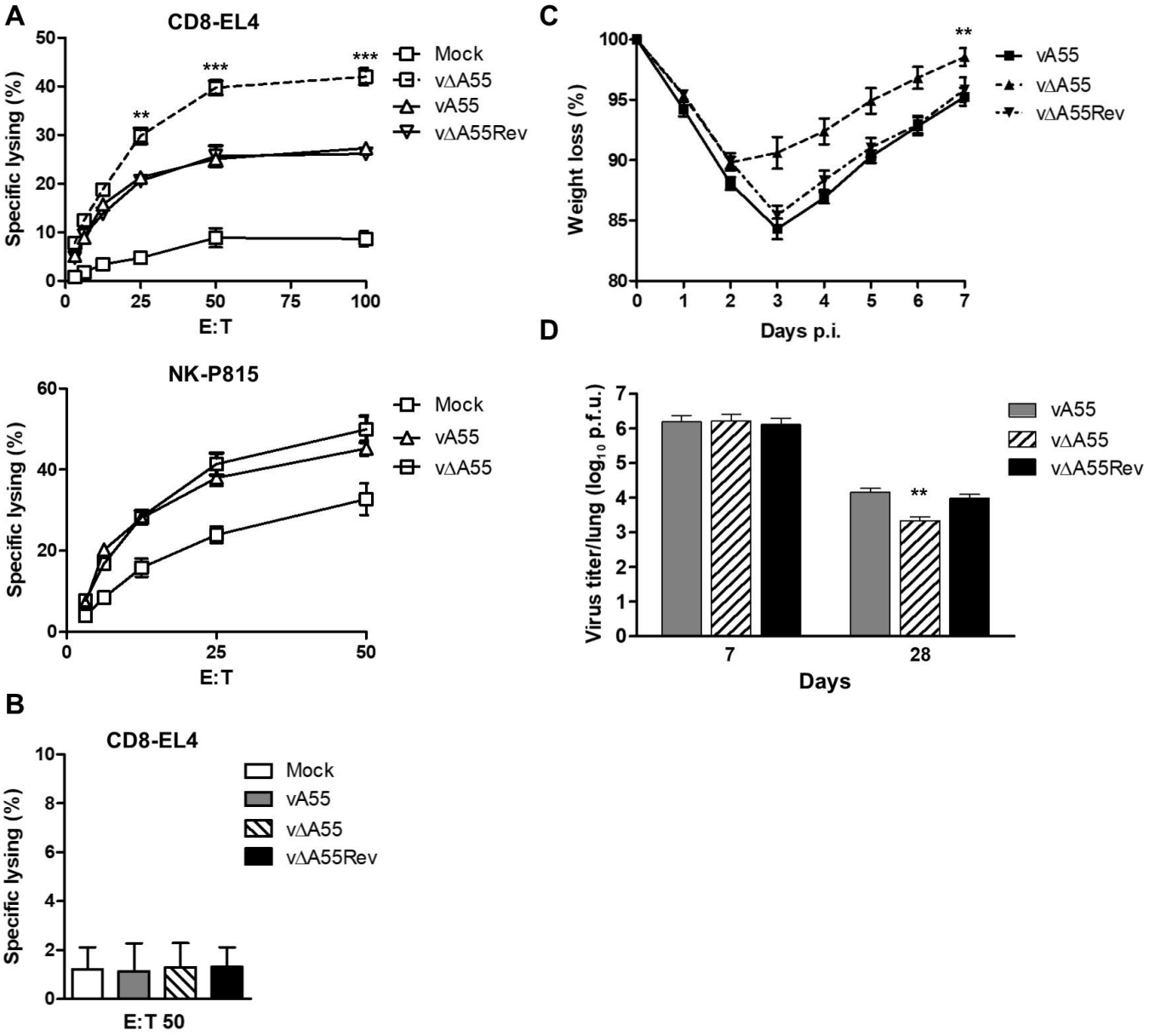
A
CD8-EL4
Specific lysing (%)
E:T
Mock
vΔA55
vA55
vΔA55Rev
**
***
***
NK-P815
Specific lysing (%)
E:T
Mock
vA55
vΔA55
B
CD8-EL4
Specific lysing (%)
E:T 50
Mock
vA55
vΔA55
vΔA55Rev
C
Weight loss (%)
Days p.i.
vA55
vΔA55
vΔA55Rev
**
D
Virus titer/lung (log10 p.f.u.)
Days
7
28
vA55
vΔA55
vΔA55Rev
**